Particle motion in weak relativistic gravitational fields

Miki Obradovic,[1,2,*] Martin Kunz,[1,†] Mark Hindmarsh,[2,‡] and Ilian T. Iliev[2,§]

[1]*Département de Physique Théorique and Center for Astroparticle Physics, Université de Genève,*
Quai Ernest Ansermet 24, CH-1211 Genève 4, Switzerland
[2]*Department of Physics and Astronomy, University of Sussex, Brighton BN1 9QH, United Kingdom*

We derive the geodesic equation of motion in the presence of weak gravitational fields produced by relativistic sources such as cosmic strings, decomposed into scalar, vector and tensor parts. To test the result, we perform the first N-body simulations with relativistic weak gravitational external fields. Our test case is a moving straight string, for which we recover the well-known result for the impulse on nonrelativistic particles. We find that the vector (gravito-magnetic) force is an essential contributor. Our results mean that it is now possible to incorporate straightforwardly into N-body simulations all weak relativistic sources, including networks of cosmic defects.

PACS numbers: 04.25.Nx, 95.75.Pq, 98.80.Cq

I. INTRODUCTION

Topological defects such as cosmic strings [1–4] are generic by-products of many inflationary models [5–8] and of grand unification [9], adding a characteristic signature to the gravitational and matter fluctuations predicted by inflation. Precision cosmic microwave background (CMB) measurements set limits on the allowed defect abundance [10–17] and thus also on inflationary models that produce defects.

There is also accurate data on the galaxy power spectrum over a wide range of scales [18], which constrain the matter perturbations. Inflation creates a nearly Gaussian spectrum of initial perturbations (see e.g., Ref. [19]), whose subsequent evolution can be computed in linear theory, and compared to the data (under assumptions about the bias, i.e., the ratio between the galaxy and matter power spectra). However, defects are localized and "active" [20] sources of gravitational fields, creating highly non-Gaussian perturbations [21–23]. For example, cosmic strings create a wake behind them as they move through matter [24,25], in which there is a planar relative overdensity of order 1 as soon as it is created. The evolution of the wake is therefore immediately nonlinear, and standard linear theory in Fourier space does not apply. The strong non-Gaussianity is very likely to impact the growth of structure and (for example) could affect the bias of the galaxy power spectrum. For this reason, we need to find ways to go beyond linear perturbation theory to calculate the matter power spectrum derived from the gravitational perturbations of defects.

One way to do so involves N-body simulations. In some early numerical work by Sornborger *et al.* [26,27] the structure of the wake induced by a single straight string

was studied by setting up a velocity kick toward the plane behind the string as the initial velocity perturbation, as derived from semianalytical predictions [1,28], verifying the predicted width of the wake, the inflow velocity of the dark matter and assumptions about the self-similarity of the solution.

However, in general defects have a complex and evolving three-dimensional structure that extends up to the horizon scale. For example, strings are not straight but form a tangled, self-intersecting and fast-moving network of infinite and closed pieces, with a characteristic length scale of about one third of the horizon scale and a characteristic speed of about a half that of light [29,30].

In order to capture the full impact of the defect perturbations on the large-scale structure, we will need to work on cosmological scales and with relativistic sources. For this we will need general relativity, both for the perturbations in the gravitational field, and the deviations to the motion that the field produces.

In this paper we derive from first principles the equation of motion (EOM) of massive particles in a perturbed Friedmann-Lemaître-Robertson-Walker (FLRW) cosmology, keeping all terms linear in the gravitational fields, including vector and tensor. This is required for relativistic sources such as topological defects, where all parts of the energy-momentum tensor are comparable in magnitude. We will then test our formalism with the help of a moving straight string, for which the impulse on passing particles is known exactly.

Finally, we perform an N-body simulation to study the growth of the wake behind the moving string, comparing with previous work using Newtonian gravity, and the impulse as an initial condition [26,27].

This paper establishes the formalism by which the effects of topological defects on the matter in the universe can be taken into account, as a necessary preliminary to nonperturbative (especially N-body) calculations of the growth of structure in cosmological models with defects.

---

*Miki.Obradovic@unige.ch
†martin.kunz@unige.ch
‡m.b.hindmarsh@sussex.ac.uk
§I.T.Iliev@sussex.ac.uk

The formalism is more general, however, and allows us to add any sources of weak relativistic gravitational fields to N-body simulations.

II. OVERVIEW OF LINEAR PERTURBATION THEORY

Very generally, given a metric $g_{\mu\nu}$ we can compute the Christoffel symbols

$$\Gamma^\mu_{\alpha\beta} = \frac{1}{2} g^{\mu\nu}(\partial_\alpha g_{\beta\nu} + \partial_\beta g_{\alpha\nu} - \partial_\nu g_{\alpha\beta}), \quad (1)$$

the curvature tensor $R_{\mu\nu}$ and thus the Einstein tensor $G_{\mu\nu}$ as well as the geodesic equation of motion,

$$\frac{d^2 x^\mu}{d\tau^2} + \Gamma^\mu_{\alpha\beta}[g_{\rho\sigma}]\frac{dx^\alpha}{d\tau}\frac{dx^\beta}{d\tau} = 0. \quad (2)$$

The gravitational field equations or Einstein equations,

$$G_{\mu\nu} = 8\pi G T_{\mu\nu}, \quad (3)$$

describe the interaction between gravity and matter, with the latter given by its energy-momentum tensor $T_{\mu\nu}$.

In general the Einstein equations are very difficult to solve, but in the limit of weak fields and small perturbations we can use linear perturbation theory around a fixed background metric [31–33]. These linearized equations then naturally decompose into irreducible components under rotations, scalars (S), vectors (V) and tensors (T). However, at higher order in perturbation theory this decomposition is no longer maintained and the different types of perturbations mix.

We will assume throughout this paper that the sources of the gravitational perturbations evolve on the background universe and are not affected by the perturbations that they generate, i.e., that their perturbations only affect the remaining constituents. This is the case for topological defects, for which we can perform the numerical simulations separately, recording the gravitational perturbations which are then self-consistently inserted into the linearized Einstein equations of the full system [34]. By running the defect and the N-body simulation in parallel and exchanging information between the two we could in principle include the so-called gravitational backreaction on the defects, but this is left for later work.

A. Metric and Christoffel symbols

We choose a background metric $a^2\eta_{\mu\nu}$, where $\eta_{\mu\nu} = \text{diag}(-1, 1, 1, 1)$ is the Minkowski metric (i.e., we only consider flat space) and a perturbation $a^2 h_{\mu\nu}$ so that the full metric with the S, V, T decomposition becomes

$$g_{\mu\nu} = a^2(\eta_{\mu\nu} + h^{(S)}_{\mu\nu} + h^{(V)}_{\mu\nu} + h^{(T)}_{\mu\nu}). \quad (4)$$

The scalar perturbations in the conformal Newtonian gauge, the vector perturbations in the *vector* gauge and the gauge invariant tensor perturbations are defined by

$$h^{(S)}_{\mu\nu} dx^\mu dx^\nu = -2\psi d\tau^2 + 2\phi\delta_{ij}dx^i dx^j, \quad (5)$$

$$h^{(V)}_{\mu\nu} dx^\mu dx^\nu = -2\Sigma_i d\tau dx^i \qquad k^i\Sigma_i = 0, \quad (6)$$

$$h^{(T)}_{\mu\nu} dx^\mu dx^\nu = h^{(T)}_{ij} dx^i dx^j \qquad h^{(T)}_{ij}k^j = h^{(T)i}_i = 0, \quad (7)$$

where τ is conformal time.

From the metric we can immediately derive the Christoffel symbols with the help of Eq. (1). Using primes ($0000' \equiv \partial_\tau$) to denote derivatives with respect to conformal time, we find

$$\begin{aligned}
\Gamma^\mu_{\alpha\beta} = \frac{1}{2a^2}[&-(h^{(S)}_{\mu\nu} - h^{(V)}_{\mu\nu} + h^{(T)}_{\mu\nu}) \\
&\times (\partial_\beta a^2\eta_{\alpha\nu} + \partial_\alpha a^2\eta_{\beta\nu} - \partial_\nu a^2\eta_{\alpha\beta}) \\
&+ \eta^{\mu\nu}(\partial_\beta[a^2(\eta_{\alpha\nu} + h^{(S)}_{\alpha\nu} + h^{(V)}_{\alpha\nu} + h^{(T)}_{\alpha\nu})] \\
&+ \partial_\alpha[a^2(\eta_{\beta\nu} + h^{(S)}_{\beta\nu} + h^{(V)}_{\beta\nu} + h^{(T)}_{\beta\nu})] \\
&- \partial_\nu[a^2(\eta_{\alpha\beta} + h^{(S)}_{\alpha\beta} + h^{(V)}_{\alpha\beta} + h^{(T)}_{\alpha\beta})])].
\end{aligned} \quad (8)$$

In particular, the zeroth component is found to be

$$\begin{aligned}
\Gamma^0_{\alpha\beta} = \frac{\acute{a}}{a}[&2\delta^0_\alpha\delta^0_\beta + \eta_{\alpha\beta} + h^{(S)}_{\alpha\beta} + h^{(V)}_{\alpha\beta} + h^{(T)}_{\alpha\beta} - 2\psi\eta_{\alpha\beta}] \\
&+ \frac{1}{2}[2\partial_\beta\psi\delta^0_\alpha + \partial_\beta\Sigma_i\delta^i_\alpha + 2\partial_\alpha\psi\delta^0_\beta + \partial_\alpha\Sigma_i\delta^i_\beta \\
&+ \partial_0(h^{(S)}_{\alpha\beta} + h^{(V)}_{\alpha\beta} + h^{(T)}_{\alpha\beta})]
\end{aligned} \quad (9)$$

and the ith component is found to be

$$\begin{aligned}
\Gamma^i_{\alpha\beta} = \frac{\acute{a}}{a}[&\delta^i_\alpha\delta^0_\beta + \delta^i_\beta\delta^0_\alpha + \Sigma_i(\delta_{ij}\delta^i_\alpha\delta^j_\beta - \delta^0_\alpha\delta^0_\beta)] \\
&- \frac{1}{2}\partial_i(h^{(S)}_{\alpha\beta} + h^{(V)}_{\alpha\beta} + h^{(T)}_{\alpha\beta}) + \acute{\phi}(\delta^i_\alpha\delta^0_\beta + \delta^i_\beta\delta^0_\alpha) \\
&+ \partial_j\phi(\delta^i_\alpha\delta^j_\beta + \delta^i_\beta\delta^j_\alpha) - \acute{\Sigma}_i\delta^0_\alpha\delta^0_\beta \\
&- \frac{1}{2}\partial_j\Sigma_i(\delta^0_\alpha\delta^j_\beta + \delta^0_\beta\delta^j_\alpha) + \frac{1}{2}\acute{h}^{(T)}_{ji}(\delta^i_\alpha\delta^0_\beta + \delta^j_\beta\delta^0_\alpha) \\
&+ \frac{1}{2}\partial_k h^{(T)}_{ji}(\delta^j_\alpha\delta^k_\beta + \delta^j_\beta\delta^k_\alpha).
\end{aligned} \quad (10)$$

B. Einstein equations

We solve the linearized Einstein equations in Fourier space where they have a simpler form. Our Fourier transform conventions are

$$f(k) = \int_{-\infty}^\infty f(x)e^{ikx}dx \qquad f(x) = \frac{1}{2\pi}\int_{-\infty}^\infty f(k)e^{-ikx}dk. \quad (11)$$

Following the formalism of Ref. [35], the Einstein equations in Fourier space can be written as

$$\phi = \frac{4\pi G}{k^2}\left(f_\rho + 3\frac{\acute a}{a}f_v\right) \qquad \psi = -8\pi G f_\pi - \phi$$

$$\Sigma_i = -\frac{16\pi G}{k^2}w_i^{(V)} \qquad \acute h_{ij}^{\prime\prime(T)} + 2\frac{\acute a}{a}\acute h_{ij}^{(T)} + k^2 h_{ij}^{(T)} = 8\pi G\tau_{ij}^{(\pi)}.$$

$$(12)$$

In these expressions we used the following elements of the energy momentum tensor $T_{\mu\nu}$:

$$f_\rho = T_{00}$$

$$f_v = \frac{i\hat k_j}{k}T_0^j$$

$$f_p = \frac{1}{3}\delta_{ij}T^{ij}$$

$$f_\pi = -\frac{3}{2k^2}\left(\hat k^i\hat k^j - \frac{1}{3}\delta_{ij}\right)T_{ij} \qquad (13)$$

$$w_i^{(V)} = (T_{0i} - \hat k_i\hat k^j T_{0j})$$

$$\tau_{ij}^{(\pi)} = (P_{il}P_{jm} - (1/2)P_{ij}P_{lm})P^{ma}P^{lb}T_{ab}$$

where hats denote unit vectors, and where we used the projection operator

$$P_{ij} = \delta_{ij} - \hat k_i\hat k_j. \qquad (14)$$

III. PARTICLE MOTION IN WEAK GRAVITATIONAL FIELDS

Evaluating the zeroth component of the geodesic equation (2) gives us an expression for the evolution of the energy of massive particles

$$\frac{\acute E}{E} = -\acute\psi - 2\partial_j\psi\acute x^j - \acute\phi\acute x_j\acute x^j - \left(\partial_j\Sigma_i + \frac{1}{2}\acute h_{ij}^{(T)}\right)\acute x^i\acute x^j$$
$$- \frac{\acute a}{a}[(1 - 2\psi + 2\phi)\acute x_j\acute x^j - 2\Sigma_i\acute x^i + h_{ij}^{(T)}\acute x^i\acute x^j]. \quad (15)$$

Using this in the i equation we find the equation of motion of massive particles in a weak gravitational field:

$$\acute x^{\prime\prime i} = \left[\acute\psi - 2\acute\phi + 2\partial_j(\psi - \phi)\acute x^j + \acute\phi\acute x_j\acute x^j + \left(\partial_j\Sigma_k + \frac{1}{2}\acute h_{ij}^{(T)}\right)\acute x^k\acute x^j\right]\acute x^i + \frac{\acute a}{a}[-1 + (1 - 2\psi + 2\phi)\acute x_j\acute x^j - 2\Sigma_j\acute x^j + h_{kj}^{(T)}\acute x_k\acute x^j]\acute x^i$$
$$- \partial_i(\psi - \phi\acute x_j\acute x^j) + \acute\Sigma_i + \partial_j\Sigma_i\acute x^j - \partial_i\Sigma_j\acute x^j - \frac{\acute a}{a}\Sigma_i(\acute x_j\acute x^j - 1) - \acute h_{ji}^{(T)}\acute x^j - \partial_k h_{ji}^{(T)}\acute x^j\acute x^k + \frac{1}{2}\partial_i h_{kj}^{(T)}\acute x^k\acute x^j. \qquad (16)$$

We notice that all types of perturbations, scalar, vector and tensor, affect the particle motion. However, to leading order for nonrelativistic particles with $\acute x \ll 1$ we find that tensor perturbations do not contribute.

Converting (16) to physical time and retaining only the leading order terms in the particle velocity we find

$$\ddot x^i + 2\frac{\dot a}{a}\dot x^i = -\frac{1}{a^2}\partial_i\psi + \frac{1}{a}\dot\Sigma_i + \frac{\dot a}{a^2}\Sigma_i. \qquad (17)$$

The second term on the left is due to the expansion of space. Although it contains $\dot x$ it needs to be taken into account as it is not suppressed by any of the metric perturbations. The first term on the right is the usual gradient of the gravitational potential which is the sum of the potential due to the particles and the scalar perturbation potential of the topological defects.[1] However, we find that vector-type metric perturbations, if they are present, affect particle motion at the same level. Thus gravito-magnetic forces can be as important as the standard scalar force for a relativistic source. This expression should be used when extending N-body codes to account for general sources of weak gravitational fields. The full result needs to be evolved if particles can reach relativistic speeds, and it

may be worthwhile to occasionally monitor the size of the next order terms.

IV. PARTICLE MOTION INDUCED BY A STRAIGHT STRING IN MINKOWSKI SPACE

In this section we will reproduce the well-known effect of a velocity kick induced by a moving straight Nambu-Goto string on a test particle, in a nonexpanding Minkowski background with $a \equiv 1$ (see Fig. 1). We compute the result by evolving Eq. (17), which illustrates the approach that we will be using in the future for the full network and verifies that we arrive at the correct answer. We show that both scalar and vector perturbations contribute significantly to the particle motion, even though in the approximation where the particle is scattered by a string coming from infinity, in the infinite time limit only the scalar contribution remains relevant.

The string Nambu Goto action is given by

$$S = -\mu\int\sqrt{-g^{(2)}}d^2\zeta, \qquad (18)$$

where μ is the string mass density, ζ^α ($\alpha = 0, 1$) are the coordinates on the world sheet traced out by the string with spacetime coordinates $X^\mu(\zeta)$, and $g^{(2)}$ is the determinant of the induced metric on the world sheet, $g_{\alpha\beta}^{(2)} = \partial_\alpha X \cdot \partial_\beta X$.

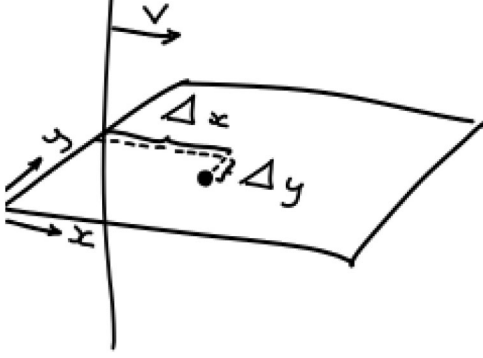The particular gauge chosen for defining the world sheet is [1]

---

[1]We allow for a nonzero anisotropic stress since for topological defects in general $\phi \neq \psi$. We note that only the ψ potential accelerates massive particles to lowest order in the particle velocity.

FIG. 1. A Nambu Goto string is aligned with the z axis and is traveling in the x direction at constant speed v through the middle of the xy plane. A test particle is at a position $(\Delta x, \Delta y)$ w.r.t. the initial position of the string such that $\Delta y / \Delta x \ll 1$. The string travels a distance $2\Delta x$.

$$g_{01}^{(2)} = 0, \qquad g_{00}^{(2)} + g_{11}^{(2)} = 0, \qquad (19)$$

and we may also identify world sheet and coordinate time with the choice $\zeta^0 = t$.

We are making the simplification of the string living in an flat, nonexpanding space. Its energy momentum tensor is [1]

$$T^{\mu\nu}(\boldsymbol{x}, t) = \mu \int d\lambda (\dot{X}^\mu \dot{X}^\nu - \acute{X}^\mu \acute{X}^\nu) \delta^{(3)}(\boldsymbol{x} - X(\lambda, t)), \qquad (20)$$

where $\dot{X}^\mu \equiv \partial_0 X^\mu$ and $\acute{X}^\mu \equiv \partial_1 X^\mu$.

We are considering specifically a straight string parallel to the z axis, traveling in the x direction at a constant velocity v^2 so that

$$\dot{X}^\mu = (1, v, 0, 0), \qquad \acute{X}^\mu = \left(0, 0, 0, \frac{1}{\gamma}\right). \qquad (21)$$

In this case we find that the energy momentum tensor is given by

$$T^{\mu\nu}(\boldsymbol{x}, t) = \gamma \mu M^{\mu\nu} \delta(x - x_0 - vt) \delta(y - y_0), \qquad (22)$$

with

$$M^{\mu\nu} = \begin{pmatrix} 1 & v & 0 & 0 \\ v & v^2 & 0 & 0 \\ 0 & 0 & 0 & 0 \\ 0 & 0 & 0 & -1/\gamma^2 \end{pmatrix}. \qquad (23)$$

We now change to Fourier space in order to solve for the perturbations in the metric with the help of the Einstein equations:

$$T^{\mu\nu}(\boldsymbol{k}, t) = 2\pi \gamma \mu M^{\mu\nu} e^{ik_x(x_0 + vt)} e^{ik_y y_0} \delta(k_z). \qquad (24)$$

$^2 v$ in units of $c = 1$, γ is the Lorentz factor.

Using Eqs. (12) with $a = 1$ we find the perturbations to be [for a detailed calculation of Eq. (28) see Appendix B]

$$\phi(\boldsymbol{k}, t) = \frac{8\pi^2 G\mu\gamma}{k^2} e^{ik_x(x_0 + vt)} e^{ik_y y_0} \delta(k_z), \qquad (25)$$

$$\psi(\boldsymbol{k}, t) = \frac{8\pi^2 G\mu\gamma}{k^2} v^2 (3\hat{k}_x^2 - 2) e^{ik_x(x_0 + vt)} e^{ik_y y_0} \delta(k_z), \qquad (26)$$

$$\Sigma_i(\boldsymbol{k}, t) = \frac{32\pi^2 G\mu\gamma}{k^2} (v_i - \hat{k}_i \hat{k}_x v) e^{ik_x(x_0 + vt)} e^{ik_y y_0} \delta(k_z), \qquad (27)$$

$$h_{ij}^{(T)} = \frac{8\pi G \tau_{ij}^{(\pi)}}{k^2 - k_x^2 v^2}. \qquad (28)$$

In our setup, we have that $v_i = (v, 0, 0)$. To calculate the effect of the perturbations on a particle to first order [Eq. (17)] we only need ψ and Σ_i. Their inverse Fourier transform is given by

$$\psi(\boldsymbol{x}, t) = \frac{G\mu\gamma v^2}{2r^2} \left[-6x^2 + r^2 \log\left(\frac{r^2}{r_0^2}\right) \right], \qquad (29)$$

$$\Sigma_1(\boldsymbol{x}, t) = \frac{2G\mu\gamma v}{r^2} \left[2x^2 - r^2 \log\left(\frac{r^2}{r_0^2}\right) \right], \qquad (30)$$

$$\Sigma_2(\boldsymbol{x}, t) = \frac{4G\mu\gamma v xy}{r^2}, \qquad (31)$$

$$\Sigma_3(\boldsymbol{x}, t) = 0, \qquad (32)$$

where r_0 is an integration constant that sets the distance at which the logarithmic contribution of the infinite straight string to ψ and Σ_1 vanishes, and $(x, y) = (x_0 + vt, y_0)$. Redefining the variables

$$x \rightarrow r_x = x - x_0 - vt, \qquad (33)$$

$$y \rightarrow r_y = y - y_0, \qquad (34)$$

Eqs. (29)–(32) give the fields at position (x, y) due to a string at $(x_0 + vt, y_0)$. Inserting these expressions into Eq. (17) we arrive, after ignoring collisions where the solution is divergent, at the following equation of motion for particles:

$$\ddot{x} = \frac{G\mu\gamma v^2}{r^4} (3r_x^2 + r_y^2) r_x, \qquad (35)$$

$$\ddot{y} = -\frac{G\mu\gamma v^2}{r^4} (3r_x^2 + 5r_y^2) r_y. \qquad (36)$$

We notice that, as expected, the logarithmically divergent part of the scalar and vector potentials ψ and Σ_i have been removed by the derivatives and the acceleration is decaying like $1/r$ at large distances. The acceleration field around a straight string is shown in Fig. 2.

We solve the equations for $x(t)$ and $y(t)$ numerically with a standard numerical solver[3] for ordinary differential equations and for initial conditions chosen so that the string passes close to a test particle in the y direction (at a distance Δy), starting at a distance Δx far away and moving past the particle in the x direction again to a distance Δx such that $\Delta y/\Delta x \ll 1$ (the nearby limit). We find that the net acceleration in the x direction cancels roughly out, while the net effect in the y direction, in particular the *velocity kick*, agrees with the predicted value [1]

$$u_{\mathrm{p}} = 4\pi G\mu\gamma v. \qquad (37)$$

Our numerical result for the effect of a GUT string with $G\mu \approx 10^{-6}$ traveling at $v = 0.333$ past a particle with $\Delta y/\Delta x \approx 0.002$ is

$$u/u_{\mathrm{p}} \approx 0.9993, \qquad (38)$$

and the agreement can be improved nearly arbitrarily as $\Delta y/\Delta x \to 0$. We also inserted the modified acceleration equations (35) and (36) into the public N-body code Gadget-2 [36] and found that the N-body code result agrees with the result from the numerical solver to machine accuracy as long as as we resolve the dynamical time of the particle string interaction in the N-body code. This can be tuned to any precision when looking at the effect on single particles (however, this may be a problem to be solved when doing large scale N-body simulations where a general small limit on the maximum time step is too expensive). We conclude that our formalism and simulation setup reproduces the standard results in nonexpanding space time accurately.

Details of the particle motion (from the N-body code) are shown in Fig. 3. The acceleration in the x direction (along the motion of the string, left panels of the figure) averages to zero, so that there is no net velocity left after the string has passed, and only a small overall displacement. It is however remarkable how the scalar and vector parts combine to a smooth overall motion, which is best visible in the middle panel on the left for the velocity in the x direction. In the y direction (perpendicular to the string motion) we can see the particle receiving the above-mentioned velocity kick. The contribution from the vector part is small and mostly serves to render the kick more step-like.

When looking in more detail at the late-time impact of the scalar and vector parts of the acceleration field, we find that in the nearby limit the vector part does not contribute significantly to the final velocity, see Fig. 4. However, this is due not least to the special case that we consider, where a long, straight string moves on a straight trajectory past a particle. In reality we will be dealing with a string network, in which case strings are not straight, and they move on
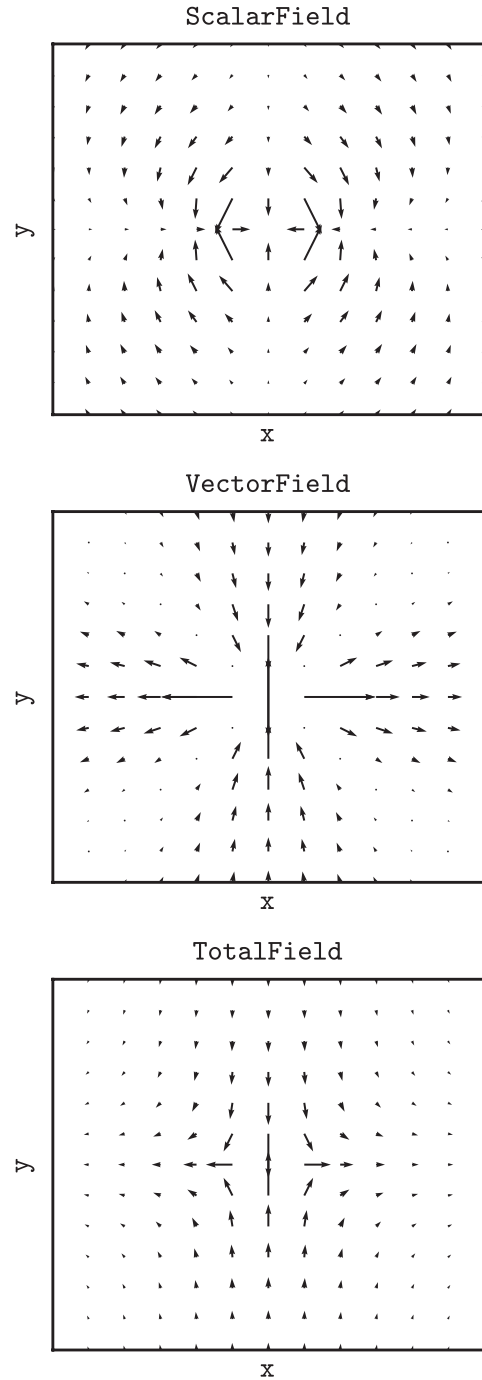
---

[3]NDSolve of the Mathematica software package.

FIG. 2. The acceleration field around a straight string in Minkowski space-time moving at constant speed in the x direction (i.e., horizontally through the center of the box). The top panel shows only the contribution from the scalar components, and the middle panel from the vector components of the metric perturbations induced by the string. The bottom panel shows the total acceleration field which is the one seen by a particle.

curved trajectories. In this case we would not expect to satisfy the nearby limit at all times. In this situation the vector part can contribute at a level comparable to the scalar part.
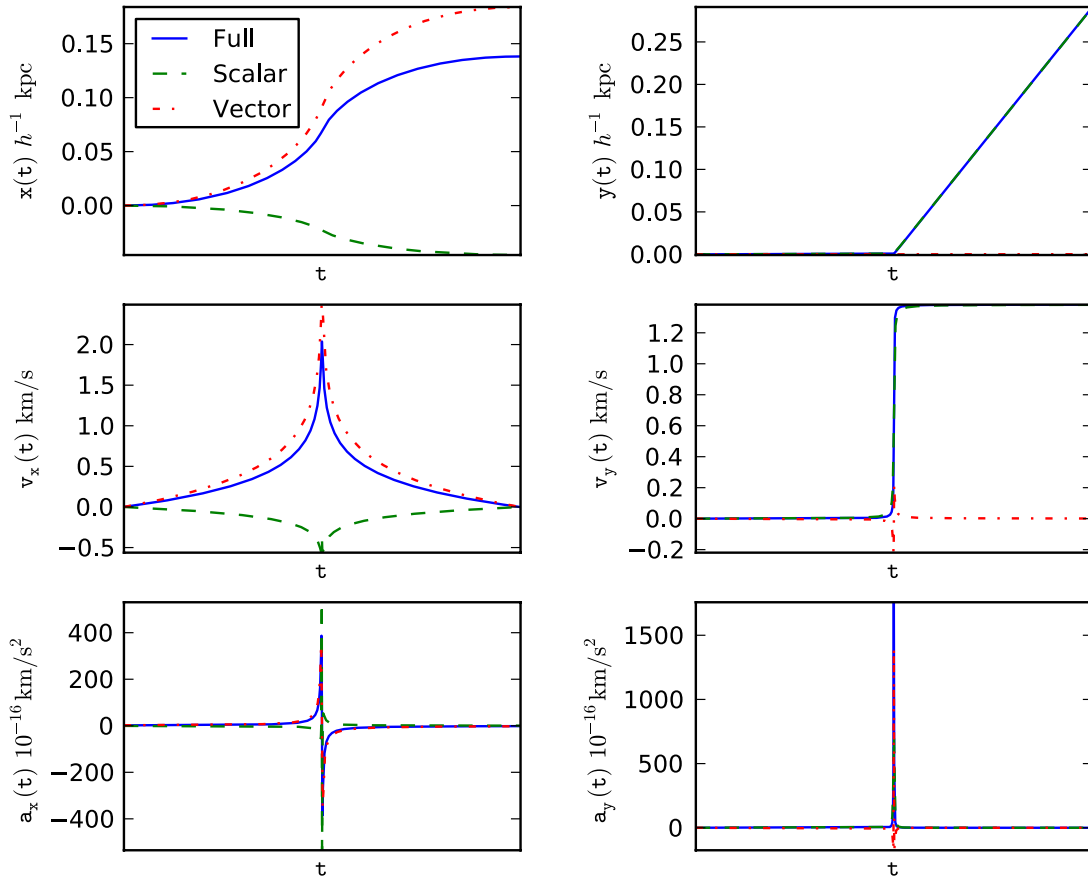
FIG. 3 (color online). Motion of a test particle in Minkowski space-time as the string passes by at a constant velocity v, from the adapted N-body code results. Initial conditions resemble the nearby limit case, i.e., the initial string particle separation is large in the x direction and small in the y direction. From the top to the bottom the panels show the particle position, velocity and acceleration. The left-hand panels show the x-component (along the direction of motion of the string) and the right-hand panels the y-component (perpendicular to the direction of motion of the string).
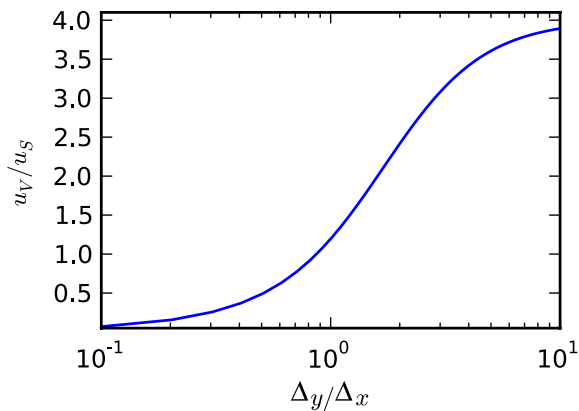

FIG. 4 (color online). Ratio of vector to scalar contributions to the final velocity in Minkowski space-time. The vector contribution is negligible in the near by limit but dominant if $\Delta y/\Delta x > 1$.

V. N-BODY RESULTS WITH A MOVING STRAIGHT STRING IN EXPANDING SPACE-TIME

We now turn to the cosmologically more relevant case of uniformly expanding space-time. Specifically, we consider an infinite, straight string moving through an initially homogeneous distribution of particles expanding with the Hubble flow and follow the subsequent evolution of those particles. We present here our leading order results and put our higher order calculations into Appendix C.

We find that the energy momentum tensor $T^{\mu\nu}$ of the Nambu-Goto string in a FLRW space-time is the same as in Minkowski space-time, except for a factor a^{-4}. This factor cancels out when calculating $T_{\mu\nu}$ which is used in the Einstein equations (12) and (13) so that

$$T_{\mu\nu}^{\text{FLRW}} = T_{\mu\nu}. \tag{39}$$

The vector and the tensor perturbations stay the same, while the scalar potentials become

$$\phi(\mathbf{k}, t) = \frac{8\pi^2 G\mu\gamma}{k^2}\left(1 - 3v\dot{a}\frac{ik_x}{k^2}\right)e^{ik_x x_s(t)}e^{ik_y y_0}\delta(k_z),$$
(40)

$$\psi(\mathbf{k}, t) = \frac{8\pi^2 G\mu\gamma}{k^2}\left(v^2(3\hat{k}_x^2 - 2) + 3v\dot{a}\frac{ik_x}{k^2}\right)$$
$$\times e^{ik_x x_s(t)}e^{ik_y y_0}\delta(k_z),$$
(41)

where $x_s(t) = x_0 + 3vt_0^{2/3}t^{1/3}$.

$\Sigma_i(\mathbf{x}, t)$ does not change (30)–(32) but $\psi(\mathbf{x}, t)$ becomes

$$\psi(\mathbf{x}, t) = \frac{G\mu\gamma v}{2r^2}\left[-6vx(t)^2 + (v - 3\dot{a}x(t))r^2 \log\left(\frac{r^2}{r_0^2}\right)\right].$$
(42)

While the logarithmically divergent contributions at small and large distances in the metric perturbations (29) and (30) did not enter the equations of motion in Minkowski space-time, we now have to deal with the term $(\dot{a}/a)\Sigma_1$. We discuss in Appendix A the (unphysical) origin of these divergences and how we regularize them, and we show that they do not influence the results.

The EOM become

$$\ddot{x} = \frac{G\mu\gamma v}{2a^2 r^4}(2vr_x(3r_x^2 + r_y^2)$$
$$+ (14r_x^2 r^2 - r^4 \log(r^2/r_0^2))\dot{a}),$$
(43)

$$\ddot{y} = -\frac{G\mu\gamma v r_y}{a^2 r^4}(v(3r_x^2 + 5r_y^2) - 7r_x r^2 \dot{a}).$$
(44)

When the string passes near a particle, this particle will be imparted a velocity towards the string (the velocity kick discussed above). In physical coordinates with the origin fixed to a point on the string trajectory, however, the particle is still following the Hubble flow until the recession velocity drops below the velocity due to the string passage. The particle will then start to move toward the region through which the string has passed, and we expect that the particles will form a wake behind the string once they reach this region. Quantitatively, we can compare the particle motion w.r.t. the axis of symmetry and the *turn-around radius* r_t at which the particle motion decouples from the Hubble flow to the calculation based on the Zel'dovich approximation in Ref. [1]: The physical particle position $y(t)$ is given by

$$y = a(y_0 + \xi/a_i),$$
(45)

where y_0 is the initial particle position and $\xi(t)$ describes its displacement,

$$\xi = -\frac{3}{5}u_i t_i\left[\frac{a}{a_i} - \left(\frac{a_i}{a}\right)^{3/2}\right]\epsilon(y_0)$$
(46)

(at late times, $a \gg a_i$, only the first term in the square brackets is relevant). We set $\epsilon(y_0) = 1$ for $y_0 > 0$ and $\epsilon(y_0) = -1$ for $y_0 < 0$ as the velocity kick is always

toward the string, u_i is the predicted velocity kick (37) and t_i, a_i are the time and scale factor at which the predicted velocity kick occurs (i.e., the moment when $x_{\text{string}} = x_{\text{particle}}$ for a particular particle). From the particle trajectory $y(t)$ it is easy to compute the turn-around radius, since at turn-around $\dot{y} = 0$. One finds that for the particle that turns around at time t,

$$r_t = -\frac{a}{a_i}\xi.$$
(47)

For testing purposes our simulation starts with a homogeneous distribution of 32^3 particles on an uniform grid in a box size of $L = 300$ kpc/h. We start at redshift $z = 99$. The string is initially at position $(-10L, L/2)$. We evolve the simulation with the string until it reaches position $(10L, L/2)$ at which point we turn it off. Thereafter we evolve only the particles and since we use these simulations to test the implementation of our formalism, we use the expansion rate of a matter dominated universe throughout as the approximation above was derived under this assumption.

Our results and comparison to the analytically-predicted trajectories and turnaround radii r_t are shown in Fig. 5. The numerically calculated particle trajectories initially follow closely the analytical predictions. Eventually the numerical results diverge from the analytical ones due to the fact that in the simulation the velocity kick for particles that are further away from the axis of symmetry is smaller than the analytically predicted velocity kick, which is derived assuming that the string that came from and went to infinity.
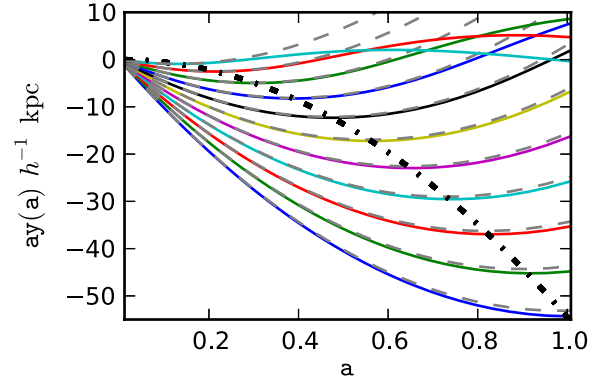
FIG. 5 (color online). Particle trajectories vs scale factor. The solid lines are the simulated particle trajectories for several sample particles at different initial distances from the passing string. The dashed lines show the corresponding trajectories based on the analytical predictions. The thick dash dotted line is the analytically-predicted turnaround radius. The analytic trajectories approach the axis of symmetry faster due to the fact that analytically all particles are treated as obeying the nearby approximation. Their velocity kick is hence larger than the one calculated in the simulation. Furthermore, in the simulation we can see the second turnaround as the particles fall back into the wake.
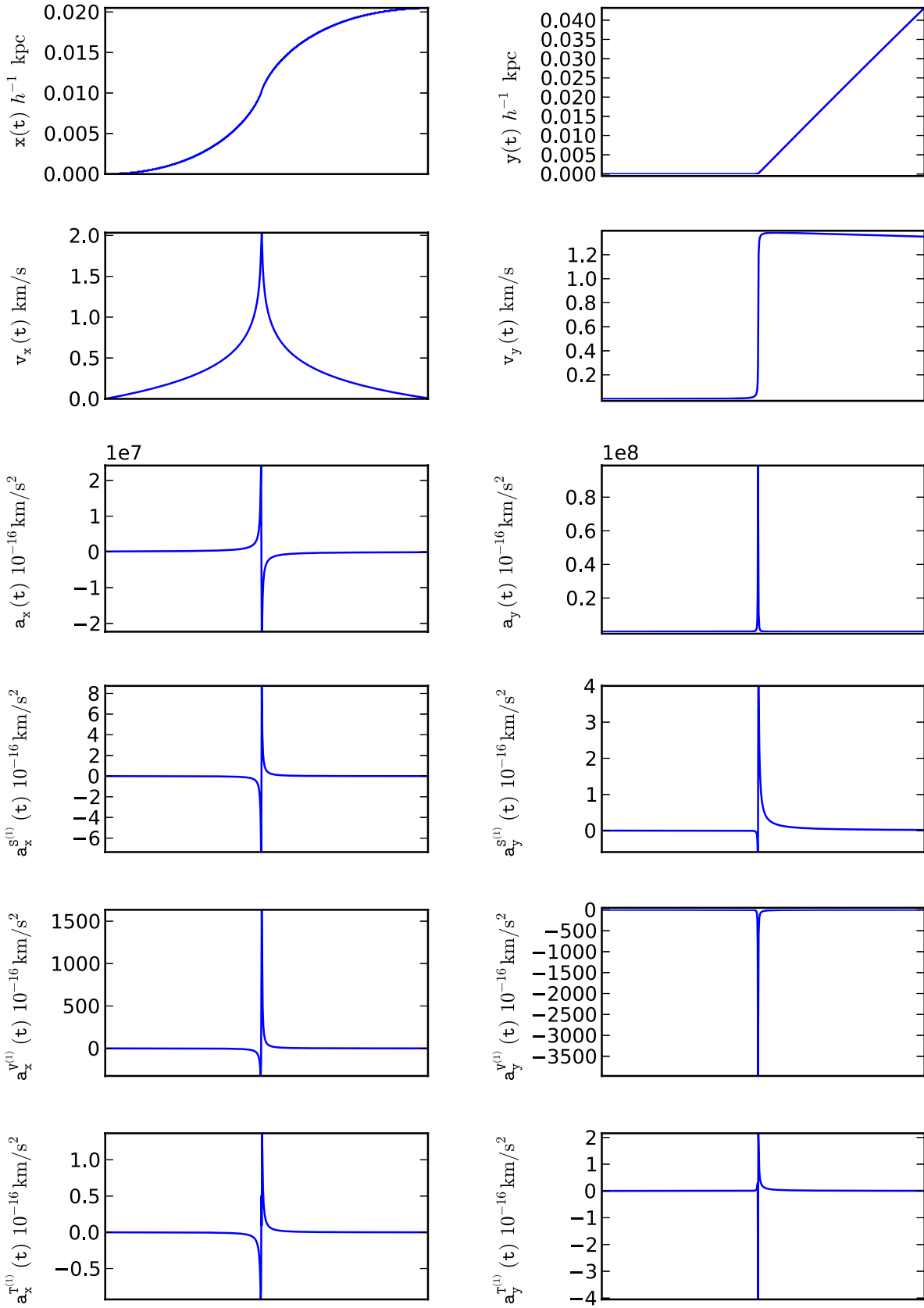
FIG. 6 (color online).　　Motion of a test particle in FLRW space-time with the same initial conditions as in Sec. V. From the top to the bottom the panels show the comoving particle position, physical velocity and comoving accelerations. The third row shows the total comoving acceleration and the rows below show the first order scalar, vector and tensor contributions to it.

VI. CONCLUSION AND OUTLOOK

In this paper we set up the formalism needed to include topological defects and other sources of weak gravitational fields in N-body simulations. For this purpose, we have derived the equations of motion of massive particles [Eq. (16)] in a perturbed background. We find that both scalar and vector (gravito-magnetic) perturbations contribute significantly to leading order, $(\dot{x}^i/c)^0$.

Tensor perturbations on the other hand do not contribute to leading order, and their contribution to the acceleration is suppressed by one power of $\dot{x}^i/c$ (we investigate the impact of the tensor perturbations in Appendix C).

To test and illustrate the equations, we have applied the leading order result [Eq. (17)] to the well-known example of a straight string. We have recovered the expected velocity kick in the limit where the string passes very close to a particle (relative to the distance that the string travels) and we have found that the vector contribution to the final particle motion is sub-dominant. Furthermore we have recovered the turn-around radii in FLRW spacetime.

Note that this is the first full numerical calculation (to first order in $\dot{x}^i$) where the velocity kick was not simply taken as an initial condition.

Our results can be used for calculating the effect of any sources of weak gravitational fields on nonrelativistic and on relativistic particles. The focus of our continuing work is on doing large scale N-body simulations and calculating the effect of Abelian Higgs cosmic string networks [37] on large scale structures.

ACKNOWLEDGMENTS

APPENDIX A: UNPHYSICAL $\log(r^2/r_0^2)$ TERM

An additional complication in the case of expanding background compared to the Minkowski space-time is evidenced by Eq. (17). Since now $\dot{a} \neq 0$, there is an additional force term proportional to Σ_i, which is logarithmically-diverging with distance to the string. This unphysical divergence arises because of the idealized nature of the infinitely long, straight Nambu-Goto string: A string of finite thickness would regularize automatically the divergence for small radii, $x^2 + y^2 \to 0$, while the divergence at large distances, $x^2 + y^2 \to \infty$ is due to the assumed infinite length of the string. This is analogous to the logarithmic divergence exhibited by the electrostatic potential of an infinite line charge. The divergence at small separations is not an issue here because the physical thickness of a realistic string is very small compared to the typical interparticle separation in a cosmological N-body simulation. However, we would expect that in a cosmological setting the size of the causal horizon would provide an upper cutoff, above which strings are not formed.

For this reason we have decided to set r_0 to horizon size and r such that $\log(r^2/r_0^2) \approx 0$ for all particles initially (we place the string initially at a distance $\sim r_0$ from the box and since $r_0 \gg L$, initially $r \approx r_0$ for all particles).

This term only affects the motion in the x direction, and hence it does not influence our results and comparison to the analytical predictions discussed above.

APPENDIX B: TENSOR PERTURBATIONS

To get the contribution due to the tensor term we solve the differential equation (12) for the tensor source

$$\tau_{ij}^{(\pi)} = \pi\gamma\mu(1 - v^2\hat{k}_x^2)\begin{pmatrix} \hat{k}_y^2 & -\hat{k}_x\hat{k}_y & 0 \\ -\hat{k}_x\hat{k}_y & \hat{k}_x^2 & 0 \\ 0 & 0 & -1 \end{pmatrix}$$
$$\times e^{ik_x(x_0+v\tau)}e^{ik_y y_0}\delta(k_z). \tag{B1}$$

For a general tensor source, the numerical method involves solving the differential equation on each grid point in Fourier space, and then numerically inverse Fourier transforming the resulting $\dot{h}_{ij}$ which is used in the equation of motion.

However, in the case of the Nambu-Goto string we directly solve the differential equation analytically for modes that are well inside the horizon, i.e., $k\tau \gg 1$. Dropping the friction term (note that this term also disappears in Minkowskian spacetime) we can rewrite it to read

$$h''^{(T)}_{ij} + k^2 h_{ij}^{(T)} = S e^{ik_x v\tau} \tag{B2}$$

where we define and use $S e^{ik_x v\tau} = 8\pi G \tau_{ij}^{(\pi)}$ to make the time dependence explicit. Hence

$$h_{ij}^{(T)} = \frac{S e^{ik_x v\tau}}{k^2 - k_x^2 v^2} + h_{ij,0,}^{(T)} \tag{B3}$$

where $h_{ij,0}^{(T)}$ is a solution to the homogeneous equation $h''^{(T)}_{ij} + k^2 h_{ij}^{(T)} = 0$, determined by the initial conditions.

Equation (B3) represents the tensor part of the boosted static gravitational field of the string when $h_{ij,0}^{(T)} = 0$. Hence we arrive at our solution

$$h_{ij}^{(T)} = \frac{S e^{ik_x v\tau}}{k^2 - k_x^2 v^2}, \tag{B4}$$

$$h'^{(T)}_{ij} = ik_x v \frac{S e^{ik_x v\tau}}{k^2 - k_x^2 v^2}. \tag{B5}$$

We also find the analytic solution to the full differential equation (12) for the tensor source (B1)

$$\tilde{h}_{ij}^{(T)} = \frac{Se^{ik_x v\tau}(-8ik_x v - 8k_x^2 v^2\tau + 4ik_x v(-k^2 + k_x^2 v^2)\tau^2 + (k^2 - k_x^2 v^2)^2\tau^3)}{(k^2 - k_x^2 v^2)^3\tau^3}. \tag{B6}$$

However, we find that $1 - |\tilde{h}_{ij}^{(T)}/h_{ij}^{(T)}| \approx 10^{-15}$ when comparing over our ranges and scales of interest $(0.01 < a < 1, \quad 2\pi/L < k_i < 512\pi/L)$ for which $1.7 \times 10^4 < k\tau < 4.4 \times 10^4$.

APPENDIX C: EQUATIONS OF MOTION TO FIRST ORDER IN THE VELOCITY

The equation of motion to first order in the particle velocities, in physical time, is

$$\ddot{x}^i + 2\frac{\dot{a}}{a}\dot{x}^i = -\frac{1}{a^2}\partial_i\psi + \frac{1}{a}\dot{\Sigma}_i + \frac{\dot{a}}{a^2}\Sigma_i + (\dot{\psi} - 2\dot{\phi})\dot{x}^i$$
$$+ \frac{1}{a}(\partial_j\Sigma_i - \partial_i\Sigma_j)\dot{x}^j - \dot{h}_{ij}^{(T)}\dot{x}^j. \tag{C1}$$

We find that all the contributions to first order in the particle velocity are significantly smaller (suppressed by one power of $(\dot{x}^i/c)$) and they hence do not influence the result (see Fig. 6). For completeness we list here all the additional first order analytical results.

The first order scalar contributions are given by

$$\dot{\psi} - 2\dot{\phi} = \frac{G\mu\gamma}{2r^4}\{(v - \dot{x})(-2r_x[4r^2 + v^2(-5r^2 + 6r_x^2)]$$
$$+ 9r^2v\dot{a}[2r_x^2 + r^2\log(r^2/r_0^2)])$$
$$+ 2r_y\dot{y}[4r^2 + v^2(r^2 + 6r_x^2) - 9r^2vr_x\dot{a}]\}. \tag{C2}$$

The first order vector contributions are given by

$$\partial_j\Sigma_1\dot{x}^j = -4G\mu\gamma v[r_x\dot{x}(r_x^2 - r_y^2) + r_y\dot{y}(3r_x^2 + r_y^2)]/r^4, \tag{C3}$$

$$\partial_j\Sigma_2\dot{x}^j = -4G\mu\gamma v[(r_x^2 - r_y^2)(r_x\dot{x} + r_y\dot{y})]/r^4, \tag{C4}$$

$$(\partial_j\Sigma_1 - \partial_1\Sigma_j)\dot{x}^j = -8G\mu\gamma vr_y\dot{y}/r^2, \tag{C5}$$

$$(\partial_j\Sigma_2 - \partial_2\Sigma_j)\dot{x}^j = 8G\mu\gamma vr_y\dot{x}/r^2. \tag{C6}$$

Note that the first two of these terms come from the $\dot{\Sigma}_i \equiv (d/dt)\Sigma_i(t, x(t), y(t))$ term.

The first order tensor contributions are given by inverse Fourier transforming Equation (B5)

$$\dot{h}_{11}^{(T)} = -G\mu\gamma vr_x(-r_x^2 + r_y^2)/r^4, \tag{C7}$$

$$\dot{h}_{22}^{(T)} = G\mu\gamma vr_x(r_x^2 + 3r_y^2)/r^4, \tag{C8}$$

$$\dot{h}_{33}^{(T)} = -2G\mu\gamma vr_x/r^2, \tag{C9}$$

$$\dot{h}_{21}^{(T)} = G\mu\gamma vr_x(r_x^2 - r_y^2)/r^4. \tag{C10}$$

Finally, note that in Eq. (16) there are further terms of order $(\dot{x}^i/c)^2$ and $(\dot{x}^i/c)^3$ which will be smaller yet.

[1] A. Vilenkin and E. P. S. Shellard, *Cosmic Strings And Other Topological Defects* (Cambridge University Press, Cambridge, England, 1994).

[2] M. Hindmarsh and T. Kibble, Rep. Prog. Phys. **58**, 477 (1995).

[3] M. Sakellariadou, Lect. Notes Phys. **718**, 247 (2007).

[4] E. J. Copeland and T. Kibble, Proc. R. Soc. A **466**, 623 (2010).

[5] J. Yokoyama, Phys. Rev. Lett. **63**, 712 (1989).

[6] A. D. Linde, Phys. Rev. D **49**, 748 (1994).

[7] E. J. Copeland, A. R. Liddle, D. H. Lyth, E. D. Stewart, and D. Wands, Phys. Rev. D **49**, 6410 (1994).

[8] M. Sakellariadou, Lect. Notes Phys. **738**, 359 (2008).

[9] R. Jeannerot, J. Rocher, and M. Sakellariadou, Phys. Rev. D **68**, 103514 (2003).

[10] N. Bevis, M. Hindmarsh, and M. Kunz, Phys. Rev. D **70**, 043508 (2004).

[11] N. Bevis, M. Hindmarsh, M. Kunz, and J. Urrestilla, Phys. Rev. Lett. **100**, 021301 (2008).

[12] J. Urrestilla, N. Bevis, M. Hindmarsh, M. Kunz, and A. R. Liddle, J. Cosmol. Astropart. Phys. 07 (2008) 010.

[13] M. Hindmarsh, Prog. Theor. Phys. Suppl. **190**, 197 (2011).

[14] R. A. Battye, B. Garbrecht, and A. Moss, J. Cosmol. Astropart. Phys. 09 (2006) 007.

[15] R. Battye, B. Garbrecht, and A. Moss, Phys. Rev. D **81**, 123512 (2010).

[16] R. Battye and A. Moss, Phys. Rev. D **82**, 023521 (2010).

[17] M. Landriau and E. Shellard, Phys. Rev. D **67**, 103512 (2003).

[18] B. A. Reid *et al.*, Mon. Not. R. Astron. Soc. **404**, 60 (2010).

[19] A. R. Liddle and D. H. Lyth, *The Primordial Density Perturbation: Cosmology, Inflation and the Origin of Structure* (Cambridge University Press, Cambridge, England, 2009).

[20] A. Albrecht and A. Stebbins, Phys. Rev. Lett. **68**, 2121 (1992).

[21] M. Hindmarsh, C. Ringeval, and T. Suyama, Phys. Rev. D **80**, 083501 (2009).

[22] M. Hindmarsh, C. Ringeval, and T. Suyama, Phys. Rev. D **81**, 063505 (2010).

[23] C. Ringeval, arXiv:1005.4842.

[24] A. Stebbins, S. Veeraraghavan, J. Silk, R. Brandenberger, and N. Turok, Astrophys. J. **322**, 1 (1987).

[25] T. Hara and S. Miyoshi, Prog. Theor. Phys. **77**, 1152 (1987).

[26] A. Sornborger, R. Brandenberger, B. Fryxell, and K. Olson, Astrophys. J. **482**, 22 (1997).

[27] A. Sornborger, Phys. Rev. D **56**, 6139 (1997).

[28] J. Silk and A. Vilenkin, Phys. Rev. Lett. **53**, 1700 (1984).

[29] M. Hindmarsh, S. Stuckey, and N. Bevis, Phys. Rev. D **79**, 123504 (2009).

[30] J. Moore, E. Shellard, and C. Martins, Phys. Rev. D **65**, 023503 (2001).

[31] H. Kodama and M. Sasaki, Prog. Theor. Phys. Suppl. **78**, 1 (1984).

[32] V. F. Mukhanov, H. Feldman, and R. H. Brandenberger, Phys. Rep. **215**, 203 (1992).

[33] C.-P. Ma and E. Bertschinger, Astrophys. J. **455**, 7 (1995).

[34] R. Durrer, *Fundamentals of Cosmic Physics* (1994).

[35] R. Durrer, M. Kunz, and A. Melchiorri, Phys. Rep. **364**, 1 (2002).

[36] V. Springel, Mon. Not. R. Astron. Soc. **364**, 1105 (2005).

[37] N. Bevis, M. Hindmarsh, M. Kunz, and J. Urrestilla, Phys. Rev. D **75**, 065015 (2007).